Localized Tungsten Deposition in Divertor Region in JT-60U

Y. Ueda 1), M. Fukumoto 1), J. Watanabe 1), Y. Ohtsuka, 1), T. Arai 2), N. Asakura 2), Y. Nobuta 2), M. Sato 2), T. Nakano 2), J. Yagyu, 2), K. Ochiai 3), K. Takakura 3), T. Tanabe 4), and JT-60 Team

1) Graduate School of Engineering, Osaka University, Suita, Osaka 565-0871, Japan
2) Japan Atomic Energy Agency, Mukouyama, Naka, Ibaraki-ken 311-0193, Japan
3) Japan Atomic Energy Agency, Tokai-mura, Naka, Ibaraki-ken 319-1195, Japan
4) Interdisciplinary Graduate School of Engineering Science, Kyusyu University, Hakozaki, Fukuoka 812-8581, Japan

e-mail contact of main author: yueda@eei.eng.osaka-u.ac.jp

Abstract. Deposition profiles of tungsten released from the outer divertor were studied in JT-60U. A neutron activation method was used for the first time to accurately measure deposited tungsten. Surface density of tungsten in the thick carbon deposition layer can be measured by this method. Tungsten was mainly deposited on the inner divertor (around inner strike points) and on the outer wing of the dome. Toroidal distribution of the W deposition was significantly localized near the tungsten released position, while other metallic impurities such as Fe, Cr, Ni were distributed more uniformly. These data indicate that inward drift in the divertor region played a significant role in tungsten transport in JT-60U.

1. Introduction

Tungsten is a leading candidate for plasma facing materials of divertors and armour materials of blankets. However, accumulation of tungsten in core plasmas leading to enhancement of radiation loss is a major concern. Therefore, understanding and appropriate control of tungsten erosion and transport are important to prove compatibility of tungsten walls with high performance plasmas. Erosion and transport of high Z materials have been studied in several tokamak devices such as ASDEX-U [1] and Alcator C-Mod [2]. Although many important results have been found in these experiments, plasma confinement and stored energy of these devices are quite different from those of ITER. In addition, detailed measurements of tungsten transport in SOL plasmas have been lacking. Therefore, more research works are necessary, especially on local tungsten transport in large confinement devices. In this study, redeposition profile of W released from the outer divertor was studied in JT-60U and it was found that tungsten transport in divertor region was strongly affected by the inward drift.

2. Experiment

In the experimental campaigns 2003-2004 (1^{st}) and 2005-2006 (2^{nd}) in JT-60U, 12 tungsten-coated CFC tiles (10 tiles for the 2^{nd} campaign) were installed in the outer divertor (section P-8). Tungsten coating (50 μm thickness) was made by the vacuum plasma spray (VPS) method with W/Re multi-interlayers. This tile array covered about 1/21 toroidal length. The W tile position in the poloidal plane is shown in Fig. 1. A photograph of the tungsten tile array before plasma exposure is shown in Fig. 2. Although some of discharges (2-3% of total number) had outer strike points on the W-tiles, most of tungsten erosion took place without the strike points on the W tiles. Effective sputtering yield of the W tiles was evaluated to be roughly 10^{-4}, similar to the results of ASDEX-U [3].

In the last 13 shots in the 1st campaign (NBI heated, L-mode), ^{13}C marked methane was puffed between the outer divertor CFC tiles (see Fig.2) to study carbon migration in JT-60U.

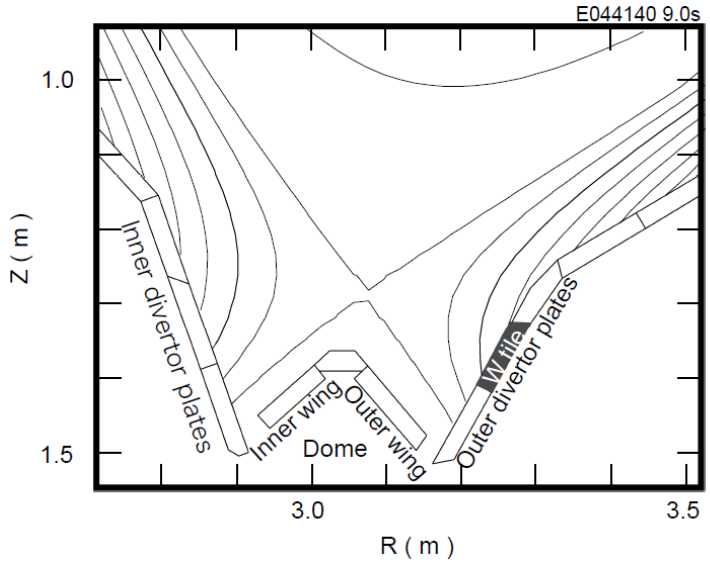

Fig.1 Magnetic surface of JT-60U divertor. W tiles were installed in the outer divertor.

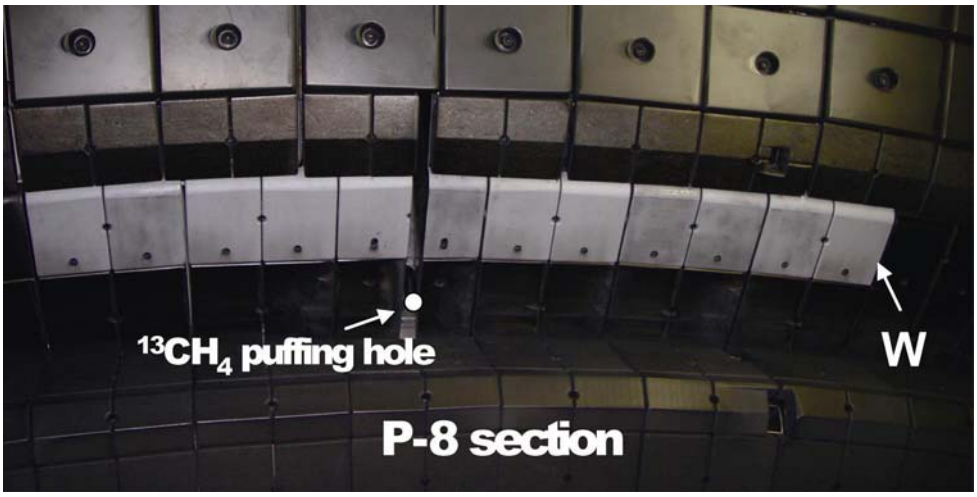

Fig.2 Photo of tungsten coated tiles installed in the outer divertor in the P-8 section . The location of a $^{13}CH_4$ gas puff hole is also shown.

The ^{13}C methane puffing resulted in very thick deposition layers (> 200 μm) on the adjacent outer divertor tiles and thick deposition layers (~10 μm, mixed with normal carbon ^{12}C) on the inner divertor tiles near the inner strike points.

After the 1st campaign, ferritic steel tiles were installed on the outer first walls to reduce toroidal field ripples. These ferritic steel tiles contain about 2 at% tungsten. Therefore, tungsten sputtered from these tiles affected tungsten deposition in the 2nd campaign. Since these tiles were almost uniformly distributed (set at intervals) in the toroidal direction, deposition of W from these tiles is considered to be toroidally uniform on the divertor tiles.

Absolute surface density of deposited tungsten was measured mainly by a neutron activation method for the first time. The $^{186}W(n,\gamma)^{187}W$ reaction by slow neutrons in JAEA/FNS (Fusion Neutronics Source) was used [4]. The produced isotope ^{187}W was radioactive with the half life of about 23.5 hours. Conventional surface analysis methods such as EDX (Energy Dispersive X ray spectrometry) and XPS (X ray photoelectron spectroscopy) were also used. As shown later, tungsten deposition on the dome tiles was found only near the top surface (within the depth of a few μm), while tungsten on the inner divertor tiles was codeposited with carbon to the depth up to about 30 μm (for the tiles removed after 1st

campaign). The neutron activation method can measure tungsten in these thick codeposition layers. Ion beam analysis such as PIXE (Particle Induced X-ray Emission) is not appropriate for this case since only near-surface tungsten (up to ~10 μm) can be precisely measured.

3. Tungsten deposition characteristics in the poloidal plane

Figure 3 shows SEM photographs of the fracture surfaces and tungsten depth profiles measured by XPS for the outer wing tile of the dome in the same toroidal section as the tungsten tile array (P-8 section). On this tile, thin carbon deposition layers up to a few tens of

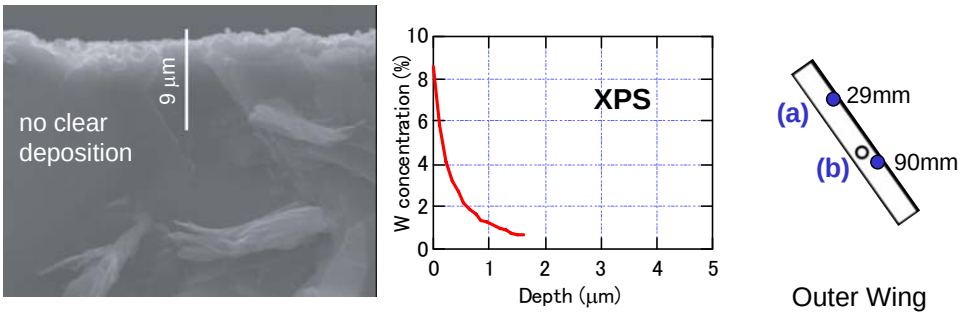

(a) Fracture and W depth profile at **29 mm**

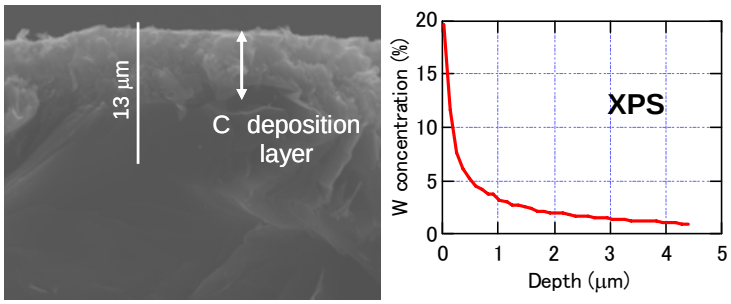

(b) Fracture and W depth profile at **90 mm**

Fig. 3 Fracture surface and W depth profile on the outer wing of the dome tile after the 1st campaign.

μm was observed. The thickness of the deposition layer increases toward the lower side of the tile (toward the outer pumping slot). Tungsten deposition was observed only in the near surface layers within the analyzing depth of EDX (~ 5μm). Therefore, EDX point analysis data for the surface of the tiles can be used to roughly evaluate the surface density of tungsten.

On the other hand, on the inner divertor tiles, very thick carbon deposition was observed, see Fig. 4. The details of these carbon deposition was reported by Gotoh et al [5]. Tungsten was codeposited with carbon to form thick mixed material layers and were embedded beneath the ^{13}C deposition layers which was the thickest near the inner strike positions. From the W depth profile (Fig.4(b)), it is clearly shown that tungsten exists in sub-surface layer, deeper than 10 μm.

Poloidal distribution of tungsten surface density was plotted in Fig. 5 together with the ^{13}C surface density profile. On the inner divertor tile, the deposition peaks of tungsten and ^{13}C are almost the same, suggesting transport mechanism to the inner divertor tile were closely correlated. According to Y. Nobuta et al. [6], the poloidal distribution of ^{13}C on the inner divertor peaked at a little outboard side from the strike point (private flux region). This peak shift could be caused by ^{13}C transport through the private flux region. On the other hand, for W deposition, all plasma shots in the 1st campaign contributed to this profile. Therefore, it is

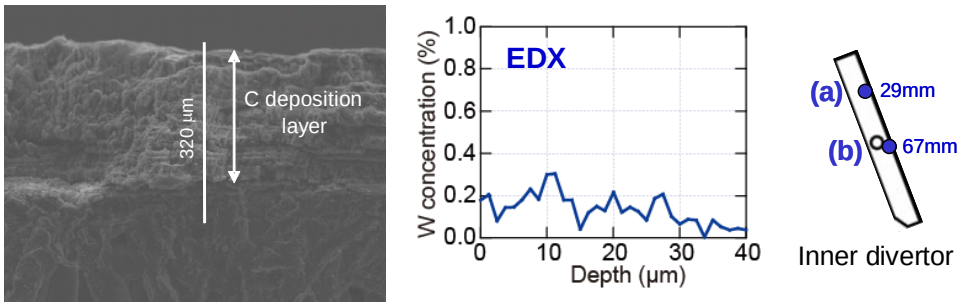

(a) Fracture and W depth profile at 29 mm

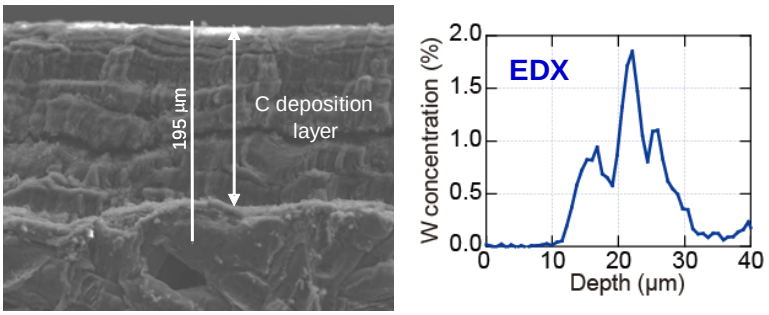

(b) Fracture and W depth profile at 67 mm

Fig. 4 Fracture surface and W depth profile on the outer wing of the dome tile after the 1st campaign. The strike points in most operations lay at around 67 mm.

hard to draw clear conclusion but at least it could be noted that some of W deposition could take place by the transport through private flux region. To compare ^{13}C and W deposition, only tungsten deposition profile has a tail on the upper end of the tile (inboard side). This

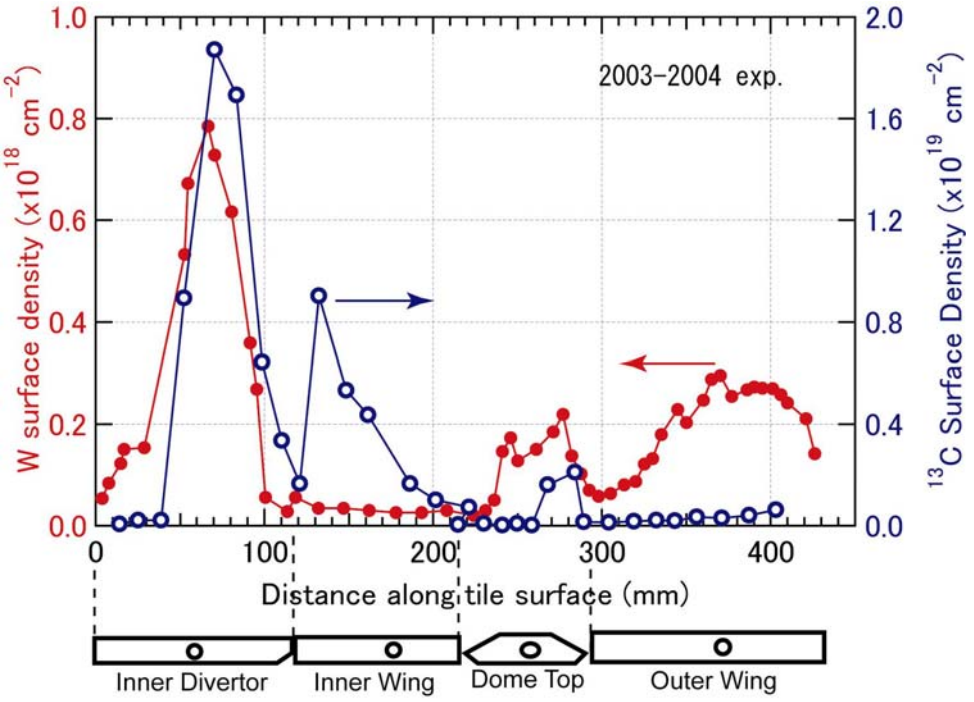

Fig. 5 Poloidal distribution of tungsten and ^{13}C surface densities in the divertor region (P-8 section) after 1st campaign (2003-2004). Surface density of W was estimated on the basis of EDX data absolutely calibrated by the neutron activation methods at 8 data points. The other points were estimated by interpolation.

deposition could be formed under the plasma operation in which the inner and outer strike points were moved up in selected 25 discharges in the 1st campaign. Concerning deposition on the dome tiles (inner wing, top, and outer wing), significant tungsten deposition was observed on the outer wing of the dome, but ^{13}C was not. On the other hand, on the inner wing of the dome, significant ^{13}C deposition was observed, but W was not. On the inner wing tile, ^{13}C deposition could be also related to the transport through the private flux region. In addition, resputtering of ^{13}C deposition layer on the inner divertor followed by deposition on the inner wing might contribute because of longer ionization length of C (or hydro-carbon) than W. For W deposition on the inner wing, both effects could be less than ^{13}C. The difference in the deposition in the outer wing could be related to the strong localization of the tungsten deposition profile in the toroidal direction, which is shown in the next section.

4. Toroidal distribution of tungsten deposition

Tungsten surface density was compared at two different toroidal positions separated by 60 deg. It was found that tungsten surface density was not the same at the different toroidal positions both in the inner divertor and the outer wing of the dome, see Fig. 6. Tungsten surface density in the both positions was much higher at 0 deg (near the W-tile position) than that at 60 deg (section P-5). Especially in the outer wing, tungsten deposition was hardly observed at 60 deg.

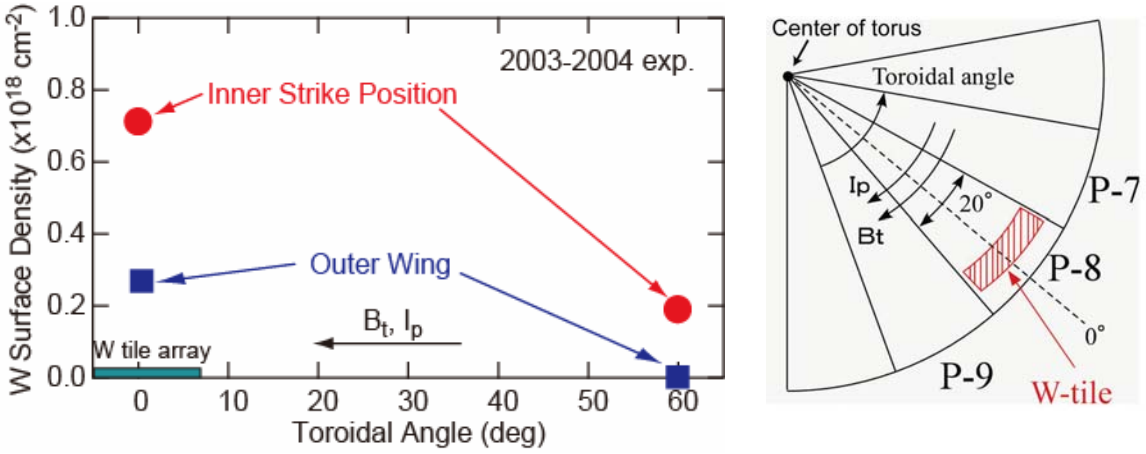

Fig. 6 W surface density measured by the neutron activation method at the inner strike position and the center of outer wing (left figure) after the 1st campaign. Definition of toroidal angle is shown in the right figure. Toroidal angle is defined as the angle viewed from the top of the torus (counter-clockwise). Toroidal angle of a single section is 20 deg. The direction of toroidal field and plasma current are clockwise.

According to Y. Nobuta et al.[5], ^{13}C ions puffed as $^{13}CH_4$ from the P-8 section (see Fig. 2) showed much longer-distant transport in the toroidal direction. They compared ^{13}C deposition on the outer wing tiles in the P-8 and P-5 sections. The ^{13}C deposition in the P-5 section was even higher than that in the P-8. This long transport of carbon ions in the toroidal direction could be partly due to plasma flow along magnetic field, since in the SOL plasma near the outer divertor the plasma flow direction was counter-clockwise. Therefore, carbon ions and tungsten ions could have different transport characteristics in the toroidal direction in the SOL plasma. But it is noted that ^{13}C marked methane puffing experiments were done under controlled L mode-discharges, while the tungsten deposition profiles was the results of various discharges during the 1st campaign. In addition, the injection position of $^{13}CH_4$ (near the strike point of the outer divertor) and the emission position of W (upper position of the

strike point) were different. So, more careful investigation would be needed to make detailed comparison of transport characteristics between carbon ions and tungsten ions.

Detailed measurement of W toroidal distribution on the outer wing is shown in Fig. 7 and Fig. 8. It is noted that these data were taken for the tiles removed after the 2nd campaign. This means tungsten erosion from the ferritic steel plates must be considered. Since the ferritic steel tiles were installed roughly uniform in the toroidal direction, materials deposition originated from these tiles could be also uniform in the divertor region. Therefore, we compared deposition profiles of several metals, some of which were originated from the ferritic tiles. Figure 7 shows toroidal distribution of W, Fe, Ni, and Cr on the outer wing of the dome. Since ferritic steel does not include Ni, this could come from some other place such as the surface of the vacuum vessel made by SUS. Toroidal distributions of Fe, Ni, and Cr are rather uniform with small dips around 0 deg. On the other hand, W distribution is very localized near the W array position. In addition, W deposition in the negative toroidal angle region is very close to none. Therefore, it could be concluded that tungsten deposition on the outer wing of the dome was hardly affected by the tungsten erosion from the ferritic steel plates.

The significant localization of tungsten deposition on the outer wing shown in Fig. 8 (the neutron activation method) is consistent with the data shown in Fig. 7 (EDX). Deposition data in Fig. 7 had some errors mainly due to surface roughness, which could be attributed to slight

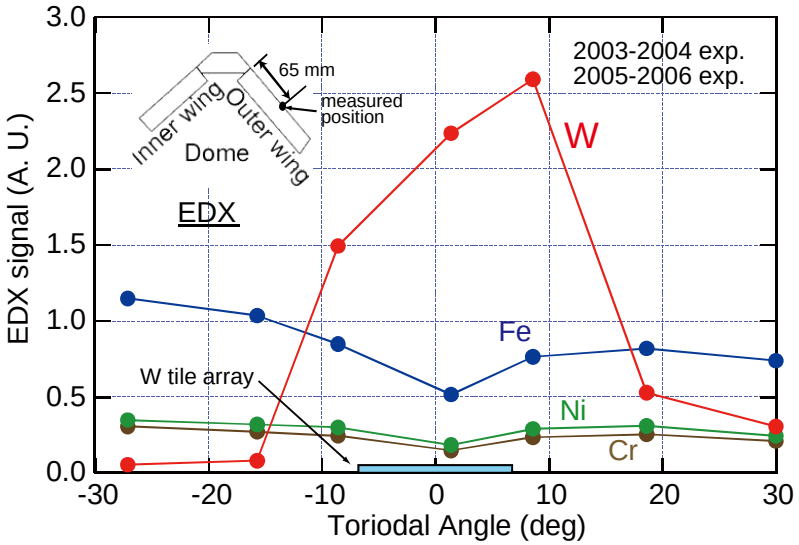

Fig. 7 Toroidal distribution of W, Fe, Cr, Ni on the outer wing (EDX results, not absolutely calibrated) after the 2nd campaign. The measured position was X = 65 mm, almost the central position of the tile. The tile length is 120 mm.

difference in the peak position between the results of the neutron activation and EDX. The peak value of the W surface density in Fig. 8 is about twice as much as that in Fig. 5. This is reasonable because the deposition in Fig. 8 took place during the 1st and 2nd campaigns, while that in Fig. 5 took place during only the 1st campaign. This also supports our conclusion that tungsten deposition originated from the ferritic steel tiles are negligible.

Both profiles (Fig. 7 and Fig. 8) show some asymmetry in the toroidal direction so that the deposition in the positive toroidal angle region is larger than that in the negative region. This could be due to the plasma flow along the magnetic field, which has the direction of increasing toroidal angle (counter-clockwise). But this effect is much less than that of ^{13}C ions, significant amount of which reached the P-5 toroidal section toroidally 60 deg away from the $^{13}CH_4$ injection point.

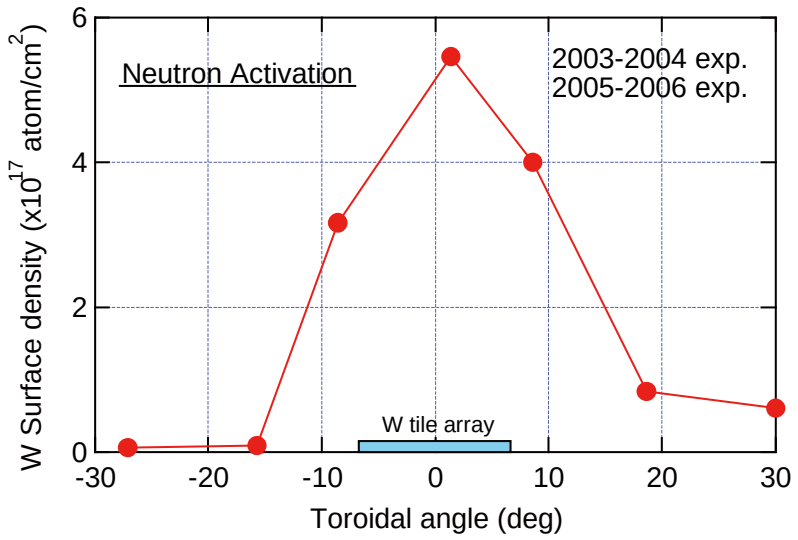

Fig. 8 Toroidal distribution of W on the outer wing (neutron activation method) after the 2nd campaign. The measured position was X = 65 mm, the same as Fig. 7.

Localized deposition of tungsten was not attributed to direct deposition of eroded tungsten atoms from the W tiles without ionization. Ionization length of tungsten atoms in the divertor plasma was more than an order of magnitude shorter than the distance between the W tiles and the outer wings. Therefore, it could be considered that tungsten transport in the outer divertor plasma was significantly affected by the inward drift. This drift could be the ExB drift driven by electric fields in the poloidal plane. The drift velocity due to the ExB drift is the same for all ions, in other words, the effect is the same for tungsten and carbon ions. But the flow velocity along magnetic field is higher for carbon ions than tungsten ions due to the difference in mass. This difference in the flow velocity could be attributed the degree of localization of the deposition profiles between tungsten and carbon.

Toroidally localized W deposition was also observed on the inner divertor tile, see Fig. 6. This could suggest that some tungsten could be also transported to the inner divertor through the private flux region. If tungsten ions are transported through the SOL around the core plasma or through the core plasma, the toroidal distribution could be more uniform. But more studies are needed to clarify impurity transport in the private region.

5. Conclusion

Tungsten local transport in the diverter region emitted from the outer divertor (mostly above the outer strike point) was studied. On the outer wing tile, W existed only in the top surface, while on the inner divertor tile W was embedded in the thick carbon deposition layer (~30 μm in the 1st campaign). Poloidal distribution in the P-8 toroidal section (W tile array position) showed dense W deposition near the inner strike point was observed. In addition, significant deposition of W was found on the outer wing of the dome. Toroidal distribution on the outer wing showed significant localization of W deposition near the W tile array. This could be attributed to inward drift. The toroidal localization of W deposition on the inner divertor was also observed. Carbon ions by puffing $^{13}CH_4$ at the same toroidal position of the W tiles were deposited also near the inner strike positions on the inner divertor tiles. In addition, ^{13}C ions were transported much longer than W ions in the toroidal direction.

References

[1] R. Neu, R. Dux, A. Kallenbach, Nucl. Fusion 45 (2005) 209.
[2] B. Goetz et al., J. Nucl. Mater. 220–222 (1995) 971.
[3] K. Ochiai, et al., to be submitted.
[4] Y. Gotoh et al., J. Nucl. Mater. 313-316 (2003) 370.
[5] K. Krieger et al., J. Nucl. Mater. 241-243 (1997) 734.
[6] Y. Nobuta et al., 34th EPS Conference on Plasma Phys. Warsaw, July (2007)